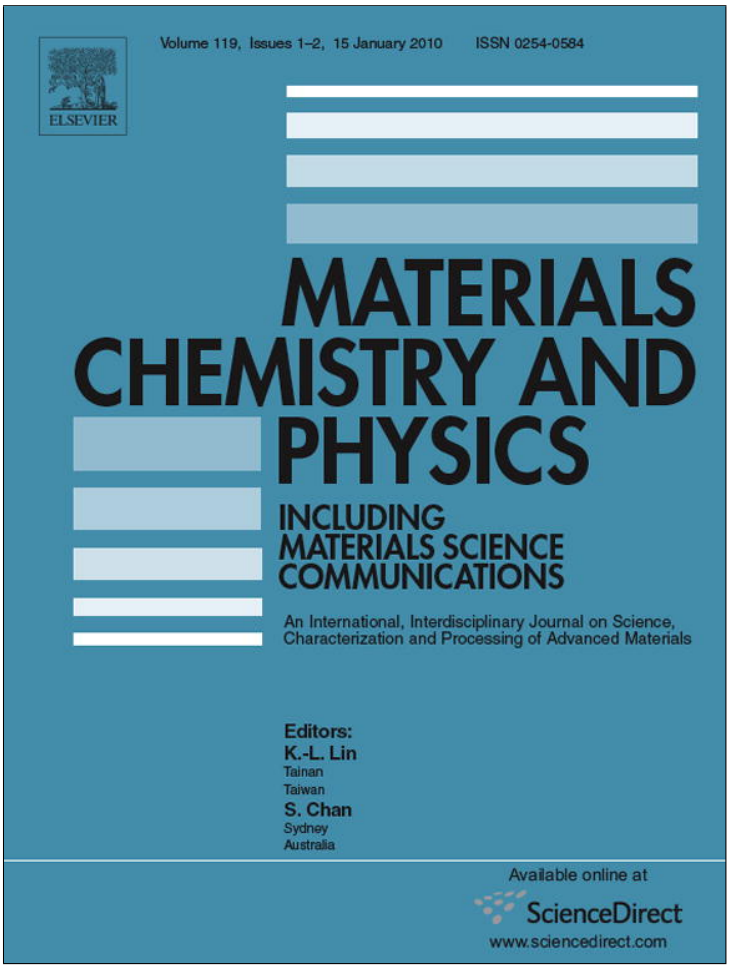

Materials Chemistry and Physics 119 (2010) 337–346

Contents lists available at ScienceDirect

Materials Chemistry and Physics

journal homepage: www.elsevier.com/locate/matchemphys

Thermal oxidation of Ti6Al4V alloy: Microstructural and electrochemical characterization

Satendra Kumar[a], T.S.N. Sankara Narayanan[a,*], S. Ganesh Sundara Raman[b], S.K. Seshadri[b]

[a] National Metallurgical Laboratory, Madras Centre, CSIR Complex, Taramani, Chennai 600 113, India
[b] Indian Institute of Technology Madras, Chennai 600 036, India

ARTICLE INFO

Article history:
Received 16 March 2009
Received in revised form 27 August 2009
Accepted 5 September 2009

Keywords:
Biomaterials
Surface modification
Electrochemical techniques
Corrosion

ABSTRACT

Thermal oxidation (TO) of Ti6Al4V alloy was performed at 500, 650 and 800 °C for 8, 16, 24 and 48 h in air. The morphological features, structural characteristics, microhardness and corrosion resistance in Ringer's solution of TO Ti6Al4V alloy were evaluated and compared with those of the untreated one. The surface morphological features reveal that the oxide film formed on Ti6Al4V alloy is adherent to the substrate at 500 and 650 °C irrespective of the oxidation time whereas it spalls off when the alloy is oxidized at 800 °C for more than 8 h. X-ray diffraction (XRD) measurement reveals the presence of Ti(O) and α-Ti phases on alloy oxidized at 500 and 650 °C, with Ti(O) as the dominant phase at 650 °C whereas the alloy oxidized at 800 °C exhibits only the rutile phase. Almost a threefold increase in hardness is observed for the alloy oxidized at 650 °C for 48 h when compared to that of the untreated one. Thermally oxidized Ti6Al4V alloy offers excellent corrosion resistance in Ringer's solution when compared to that of the untreated alloy.

1. Introduction

Titanium and titanium alloys are widely used as bio-implant materials, particularly for orthopaedic and osteosynthesis applications due to their low density, excellent biocompatibility, corrosion resistance and mechanical properties [1–4]. One of the important reasons for choosing these materials is their ability to form a stable passive oxide layer, which offers them an excellent corrosion resistance. Accumulation of ions on tissues adjacent to the implant observed during implant retrieval analysis [5] indicates that the native forms of passive oxide film (4–6 nm thick) on Ti and its alloys possess poor mechanical property and they might got disrupted at very low shear stresses, even by rubbing against soft tissues [6]. Fretting and sliding wear conditions would lead to fracture of the passive layer [7–10] and under extreme conditions cause loosening and an eventual failure of the implant. The wear debris and the metal ions released during fracture of the passive layer can cause adverse tissue reactions. These limitations preclude the use of Ti and its alloys for articulating surfaces.

Among the various types of Ti alloys, Ti6Al4V has been the choice in many instances. In spite of its good mechanical properties and corrosion resistance, the two major concerns in using this alloy for implant applications are: (i) leaching of V and Al which could cause peripheral neuropathy, osteomalacia and Alzheimer diseases when the concentration of these ions exceeds the threshold level [11–13]; and (ii) the large modulus mismatch between the Ti6Al4V alloy (~110 GPa) and the bone (~10–40 GPa), which could cause insufficient loading of the bone adjacent to the implant [14]. Insufficient loading on the bone may lead to fracture of the bone if it experiences a sudden jerk or impact due to stress shielding. Development of new alloy materials and modification of the surface of the currently used Ti alloys have been widely explored to overcome these problems. The development of Ti6Al7Nb [15] and Ti5Al2.5Fe [16], where Nb and Fe were substituted for V in Ti6Al4V alloy as less toxic alternatives have not received much success as they still contain Al [17,18]. Numerous surface modification methods such as, chemical treatment (acid and alkali treatment) [19–20], electrochemical treatment (anodic oxidation) [21], sol–gel [22], chemical vapour deposition [23], physical vapour deposition [24], plasma spray deposition [25], ion implantation [26], thermal oxidation [27], etc. have been explored to impart the desired surface properties without altering the property of the implants, especially the mechanical property and corrosion resistance, on the currently used implant materials. One of the simplest methods to generate a barrier layer on titanium is to treat it thermally in a furnace in air, which produces a surface oxide layer. Thermal oxidation (TO) treatment, which is aimed to obtain in situ ceramic coatings, mainly based on rutile, can offer thick, highly crystalline oxide films, accompanied with the dissolution of oxygen beneath them. TO of titanium and its alloys has already been investigated for biomedical applications with a focus to improve the hardness and wear resistance [28–31].

* Corresponding author. Tel.: +91 44 2254 2077; fax: +91 44 2254 1027.
E-mail address: sat_nml@rediffmail.com (S. Kumar), tsnsn@rediffmail.com (T.S.N. Sankara Narayanan).

0254-0584/$ – see front matter © 2009 Elsevier B.V. All rights reserved.
doi:10.1016/j.matchemphys.2009.09.007

The Young's modulus of thermally oxidized titanium is comparable with that of the bone [32]. However, only a few reports are available on the corrosion behaviour of thermally oxidized Ti and its alloys [27,28,33–36]. Guleryuz and Cimenoglu [27] have reported that the corrosion resistance of Ti6Al4V alloy is significantly improved after TO treatment at 600 °C for 60 h. The life time of the protective surface layer of the TO treated titanium was reported to be increased by almost 13 times than plasma nitrided titanium when it was tested in boiling 20% HCl solution [33]. According to Lopez et al. [28] Ti6Al7Nb, Ti13Nb13Zr and Ti15Zr4Nb alloys exhibited a lower current density when they are in the thermally oxidized state. Comparison of the corrosion behaviour of pickled, anodized and thermally oxidized titanium indicates that the later treatment has offered a better corrosion resistance [34,35]. Garcia-Alonso et al. [36] have reported similar corrosion behaviour of Ti6Al4V alloy when it was thermally treated at 500 and 700 °C for 1 h.

To ascertain the suitability of Ti and its alloys as an implant material, several properties must be evaluated. Among these, corrosion resistance assumes significance, because the metal ions released from the implant to the surrounding tissues may give rise to biocompatibility problems. The hardness, corrosion resistance and wear resistance are expected to improve with the formation of an adherent and hard oxide layer on the surface of titanium [33]. However, TO of Ti at high temperatures (>800 °C) and for prolonged durations of time could lead to the formation of a thick oxide layer but spallation of the oxide layer becomes a major concern [37]. The large volume ratio of rutile to Ti (1.73) [38], large lattice mismatch and the large difference in the coefficient of thermal expansion between the rutile and titanium are considered responsible for the spallation of the oxide layer [39,40]. Moreover, the nature and properties of the oxide layer would vary depending on the treatment conditions employed for oxidation. Thus, an extensive study is needed to optimize the oxidation temperature and time so as to produce an adherent surface oxide layer that can improve the corrosion resistance and biocompatibility. In terms of corrosion resistance, it is preferable to form an oxide layer with rutile structure since the rutile phase offers better corrosion resistance in hot reducing acids compared to that of the anatase phase [33]. The present study aims (i) to study the TO behaviour of Ti6Al4V alloy at different temperatures, namely, 500, 650 and 800 °C and for various durations of time, viz., 8, 16, 24 and 48 h; (ii) to evaluate the corrosion resistance of thermally oxidized Ti6Al4V alloy in Ringer's solution (simulated body fluid); and (iii) to compare the corrosion resistance of thermally oxidized Ti6Al4V alloy with that of the untreated alloy.

2. Experimental details

Ti grade-5 (chemical composition in wt.%—N: 0.02; C: 0.03; H: 0.011; Fe: 0.22; O: 0.16, Al: 6.12; V: 3.93 and Ti: balance) was used as the substrate material. Before subjecting to oxidation process, the Ti6Al4V alloy was mechanically polished using various grades of SiC paper (60, 100, 220, 320, 400, 600 and 1/0, respectively) at a very slow speed, thoroughly rinsed in deionized water and dried using a stream of compressed air. Proper care is taken during polishing so that the extent of plastic deformation will be very less to cause any significant change in the oxidation kinetics/mechanism. TO was carried out in a muffle furnace (LENTON make) at 500, 650 and 800 °C for 8, 16 and 24 h in air. The rate of heating was kept at 5 °C min^{-1} in all the experiments. Some experiments were also performed for a longer duration of 48 h at 650 °C to understand the nature of oxide layer formed at such conditions. After TO treatment, the Ti6Al4V alloy was allowed to cool in the furnace itself at its own cooling rate. Roughness measurements were performed on the surface of the Ti6Al4V alloy before and after thermal oxidation treatments using a Mitutoyo SJ-301 stylus surface profilometer. The pull off adhesion tests were performed on TO samples for the qualitative analysis of adhesion of the oxide with the substrate. The phase constituents of untreated and TO Ti6Al4V alloy and the nature of the oxide film formed on their surface were determined using X-ray diffraction (XRD) measurements (D8 DISCOVER, Bruker axs) with Cu-K_α radiation. The thickness of the oxide layer and the surface morphology of TO Ti6Al4V alloy were assessed by scanning electron microscope (SEM). The microhardness of the untreated and TO Ti6Al4V alloy was measured at the surface using a Leica VMHTMOT microhardness

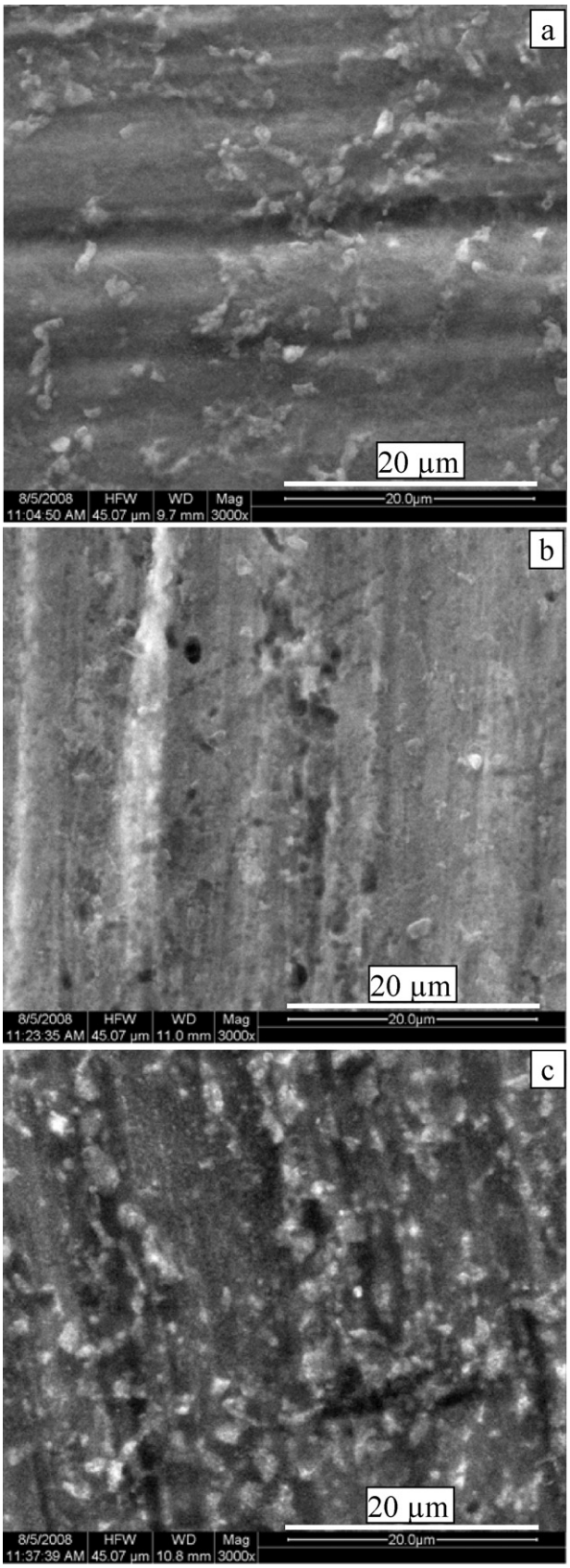

Fig. 1. Scanning electron micrographs showing surface morphology of Ti6Al4V alloy thermally oxidized at 500 °C for various durations of time in air (a) 8 h, (b) 16 h and (c) 24 h.

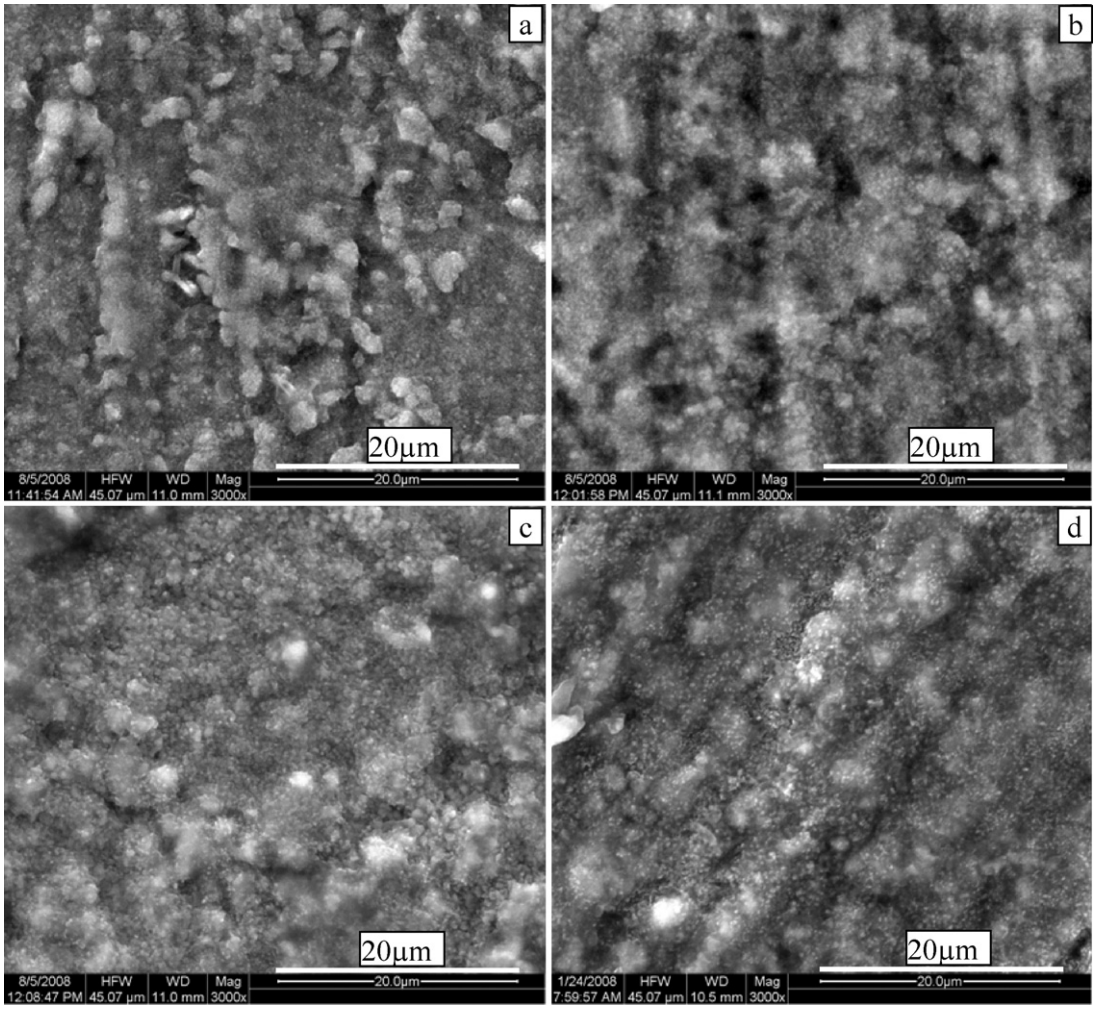

Fig. 2. Scanning electron micrographs showing surface morphology of Ti6Al4V alloy thermally oxidized at 650 °C for various durations of time in air: (a) 8 h, (b) 16 h, (c) 24 h and (d) 48 h.

tester at a load of 200 gf applied for 15 s. The microhardness depth profiles from the surface to the core of the TO Ti6Al4V alloy were also determined. Seven indentations were made on each sample and the values were averaged out.

The corrosion behaviour of untreated and TO Ti6Al4V alloy was evaluated by potentiodynamic polarization and electrochemical impedance spectroscopic (EIS) studies using a potentiostat/galvanostat/frequency response analyzer of ACM instruments (model: Gill AC). Ringer's solution, having a chemical composition (in $g\,l^{-1}$) of 9 NaCl, 0.24 $CaCl_2$, 0.43 KCl and 0.2 $NaHCO_3$ (pH: 7.8), that chemically simulates the physiological medium of the human body, which is also referred as simulated body fluid (SBF), was used as the electrolyte solution. All the experiments were conducted at 37 ± 1 °C. Before performing the corrosion studies, the untreated Ti6Al4V alloy was mechanically polished using various grades of SiC paper (60, 100, 220, 320, 400, 600, 1/0, 2/0, 3/0 and 4/0, respectively), followed by 0.3 μm alumina paste to a mirror finish, rinsed with deionized water, pickled using a mixture of 35 vol.% HNO_3, 5 vol.% HF and balance water at 40 °C, as described by Schutz and Thomas [41], thoroughly rinsed in deionized water and dried using a stream of compressed air. Ti6Al4V alloy samples subjected to TO were rinsed in deionized water and dried using a stream of compressed air. The cleaned samples, either untreated or thermally oxidized, formed the working electrode while a saturated calomel electrode (SCE) and a graphite rod served as the reference and auxiliary electrodes, respectively. These electrodes were placed in a flat cell in such a way that only 1 cm^2 area of the working electrode was exposed to the electrolyte solution.

Potentiodynamic polarization tests were carried out at a scan rate of 100 mV min^{-1} from −250 to +3000 mV vs. SCE with respect to the open circuit potential (OCP). A very high anodic potential (+3000 mV vs. SCE) was chosen to study the effect of naturally formed oxide on the untreated Ti6Al4V alloy and the oxide layer grown thermally on Ti6Al4V alloy in Ringer's solution. The corrosion potential (E_{corr}) and corrosion current density (i_{corr}) were determined from the polarization curves using Tafel extrapolation method. The passive current density (i_{pass}) corresponding to +1000 mV vs. SCE was measured from the anodic region of the polarization curve to observe the passivation ability of untreated and thermally oxidized Ti6Al4V alloy. EIS study was conducted by applying sinusoidal signal amplitude of 32 mV and the electrode response was analyzed in the frequency range between 10,000 and 0.1 Hz in Ringer's solution at their respective OCP. The impedance value of untreated and TO Ti6Al4V alloy was measured from the Bode impedance plots. The polarization and EIS studies were repeated at least 3 times to ensure reproducibility of test results.

3. Results and discussion

3.1. Visual observations

Visual observation of thermally oxidized Ti6Al4V alloy indicates the formation of a very distinct colouration on the surface. The colour of the thermally oxidized Ti6Al4V alloy changes from light blue to dark brown with the increase of temperature from 500 to 650 or 800 °C, respectively. The change in colour of the Ti6Al4V alloy after TO is due to the increase in thickness of the surface oxide layer and the consequent change in the interference of the incident light radiation. The oxide film formed at 500 and 650 °C for various durations of time is found to be adherent when evaluated by a pull off adhesion test while those formed at 800 °C for 16, 24 and 48 h exhibit spallation. Debonding of the oxide layer formed at temperatures higher than 800 °C and for longer treatment time has also been observed on CP-Ti [37,38]. Hence, further characterization was restricted only to Ti6Al4V alloy oxidized at 500 and 650 °C for 8, 16, 24 and 48 h and at 800 °C for 8 h.

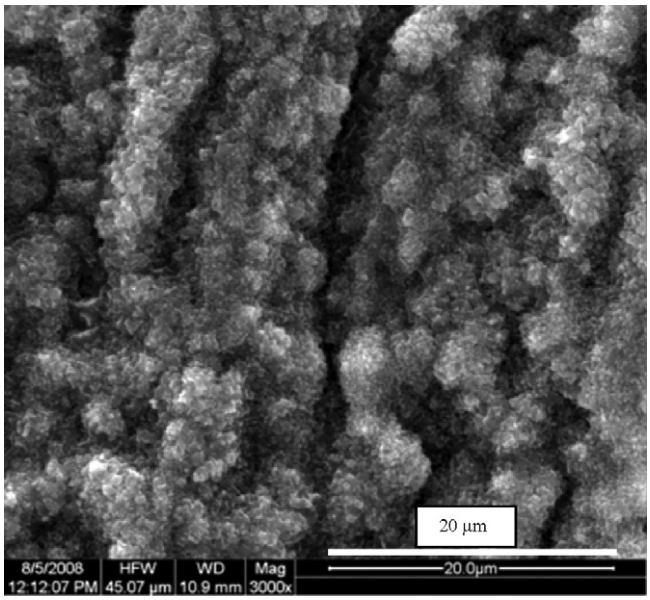

Fig. 3. Scanning electron micrograph showing surface morphology of Ti6Al4V alloy thermally oxidized at 800 °C for 8 h in air.

3.2. Surface morphology of the oxide film formed on Ti6Al4V alloy

The surface morphology of Ti6Al4V alloy thermally oxidized at 500 °C for 8, 16 and 24 h (Fig. 1), at 650 °C for 8, 16, 24 and 48 h (Fig. 2) and at 800 °C for 8 h (Fig. 3) clearly reveals the presence of oxide scales throughout the surface without spallation. A closer examination of the surface morphology of the oxide layer formed at different temperatures and for various durations of time indicates the nature of the oxide film. The surface morphology clearly reveals the formation of a thin oxide scale over the substrate along with a few nodular oxide particles when the oxidation is performed at 500 °C for 8 h. With the increase in treatment time from 8 to 16 h at 500 °C, the oxide particles grew outwardly and cover the entire surface of the alloy. However, increase in treatment time results in the increase in outward oxidation and agglomeration of the oxide, which leaves behind a gap or discontinuity of the oxide grains that could be also considered as deep grain boundary. The growth of oxide particles is found to be dependent on the temperature and it is observed that the extent of agglomeration and growth of oxide is higher at a much lower treatment time when the temperature is increased from 500 to 650 °C. In a similar way like oxidation at 500 °C, increase in treatment time at 650 °C enables an increase in the size of the oxide particles, which results in an increase in gap between the nearby oxide grains or porosity of the oxide layer. In this paper, gap between the oxides grains formed on the surface is considered as the porosity of the oxides. Finer grain size will be more compact in structure whereas bigger grains can accommodate few smaller grains between the gaps of two oxide grains. The porosity of Ti6Al4V alloy thermally oxidized at 650 °C for 16 h is higher than that oxidized at 500 °C for 16 h. Increase in treatment time from 8 to 24 h at 650 °C, results in the formation of fine and dense oxide particles, which cover the entire surface of the alloy. However, further increase in time to 48 h leads to the agglomeration of the finer oxide grains formed at lesser treatment time to a bigger one and consequently generates porosity/gap between the oxide grains on the oxide surface. The Ti6Al4V alloy thermally oxidized at 650 °C for 48 h has shown nucleation of fine particles at the gap between adjacent oxide grains. The nucleation and agglomeration of finer grains leads to the formation of bigger grains that separates with near by grains, when the oxidation temperature was increased to 800 °C and for 8 h treatment time. Increase in treatment time from 8 to 16 and 24 h at 800 °C leads to spalling off the oxide scale.

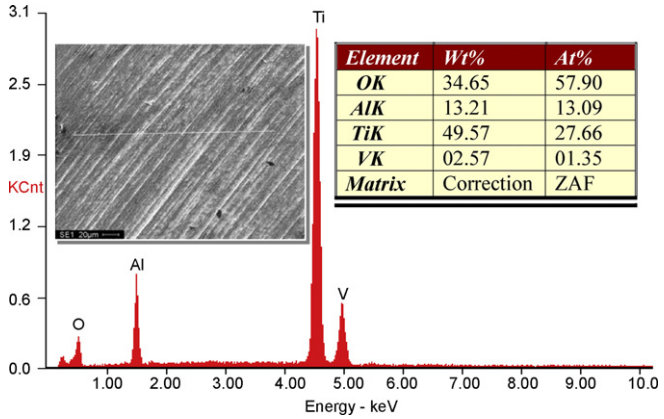

Fig. 4. EDX pattern of Ti6Al4V alloy thermally oxidized at 650 °C for 48 h. (The area used for the energy dispersive X-ray analysis and the distribution of element in that area is given in the insets.)

The evolution of surface morphology of the oxide film formed on Ti6Al4V alloy during TO at different temperatures and for various durations of time suggests that nucleation of oxide takes place throughout the surface of the samples when it immediately comes in contact with oxygen. The energy dispersive X-ray (EDX) analysis performed on a given area of Ti6Al4V alloy thermally oxidized at 650 °C for 48 h and the distribution of the elements in that area (Fig. 4) clearly reveals that the nucleation of oxide takes place throughout the surface. The growth mode involves the formation of a thin oxide scale followed by its agglomeration and growth. The cross-sectional view of samples thermally oxidized at different temperatures and times clearly reveals the presence of homogenous oxide layer over the substrate at all treatment conditions (Fig. 5).

3.3. Surface roughness of the oxide film formed on Ti6Al4V alloy

The values of surface roughness parameters (R_a, R_z and R_q) for the samples before and after TO, are given in Table 1. It is evident from Table 1 that the R_a value increases with the increase in temperature and time employed for oxidation. The increase in surface roughness of Ti6Al4V alloy following TO treatment can be ascribed to the growth mechanism of the oxide layer, i.e., with the increase in temperature and time, the kinetics of outward growth increases that has resulted in higher roughness. For any given temperature, increase in treatment time results in an increase in surface roughness. This can be explained by the fact that with increase in treatment time the oxide layer becomes porous and develops a stratified structure, which enables an increase in the surface roughness [42,43]. Borgioli et al. [44] have also reported an increase in R_a

Table 1
Surface roughness of untreated and thermally oxidized Ti6Al4V alloy.

Treatment temp. (°C)	Time (h)	R_a (μm)	R_z (μm)	R_q (μm)
Untreated	0	0.15	0.80	0.19
500	8	0.19	1.20	0.24
	16	0.23	1.82	0.30
	24	0.28	1.83	0.35
650	8	0.27	1.87	0.33
	16	0.32	2.17	0.41
	24	0.37	2.61	0.47
	48	0.43	2.97	0.54
800	8	0.60	4.05	0.75

value from 0.50 to 1.0 μm when Ti6Al4V alloy is subjected to TO at 1000 °C for 2 h in air atmosphere at 10^5 Pa.

3.4. Structural characteristics of untreated and thermally oxidized Ti6Al4V alloy

The XRD patterns of untreated and TO Ti6Al4V alloy are shown in Fig. 6. Untreated Ti6Al4V alloy is comprised of α + β phase (denoted as 'α-Ti' and β-Ti in Fig. 6). Since the depth of penetration of Cu-K_α radiation is in the range of 10–20 μm, the presence of α-Ti and α/β-Ti peaks in the XRD pattern of TO Ti6Al4V alloy with thinner oxide layer is quite evident. The XRD patterns of TO Ti6Al4V alloy exhibit the presence of rutile and oxygen diffused Ti (Ti(O)) as the predominant phase along with a small amount of α-Ti and α/β-Ti peaks. Anatase phase peaks (denoted as 'A' in Fig. 6) were also observed at lower diffraction angle for the Ti6Al4V alloy that is thermally oxidized at lower temperature such as 500 °C, irrespective of the treatment time. The intensity of the peak pertaining to the anatase phase is relatively higher at lower treatment time of 8 h along with the Ti and Ti(O) phase peaks. However, with increase in treatment time from 8 to 24 h, the intensity of the anatase peaks reduces with a concurrent increase in Ti/Ti(O) peaks. The Ti6Al4V alloy samples oxidized at 500 and 650 °C show predominantly the Ti and Ti(O) peaks whereas those oxidized at 800 °C show only the rutile phase (denoted as 'R' in Fig. 6). Similar observations were also made earlier by other researchers [27,28,31,36,45]. Siva Rama Krishna et al. [31] have reported the formation of Ti(O) at temperatures less than 700 °C and rutile at and above 800 °C as the dominant phase following oxidation of titanium. Guleryuz and Cimenoglu [27,45] have reported the presence of anatase phase when the Ti6Al4V alloy was oxidized at 600 °C for 24 and 48 h whereas rutile was

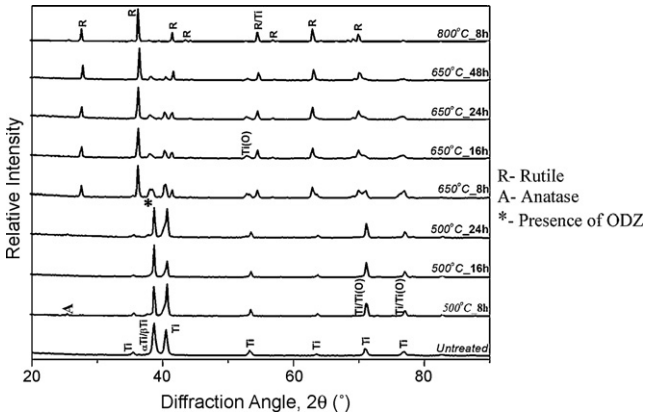

Fig. 6. XRD patterns of untreated Ti6Al4V alloy and samples thermally oxidized at different temperatures for various durations of time in air.

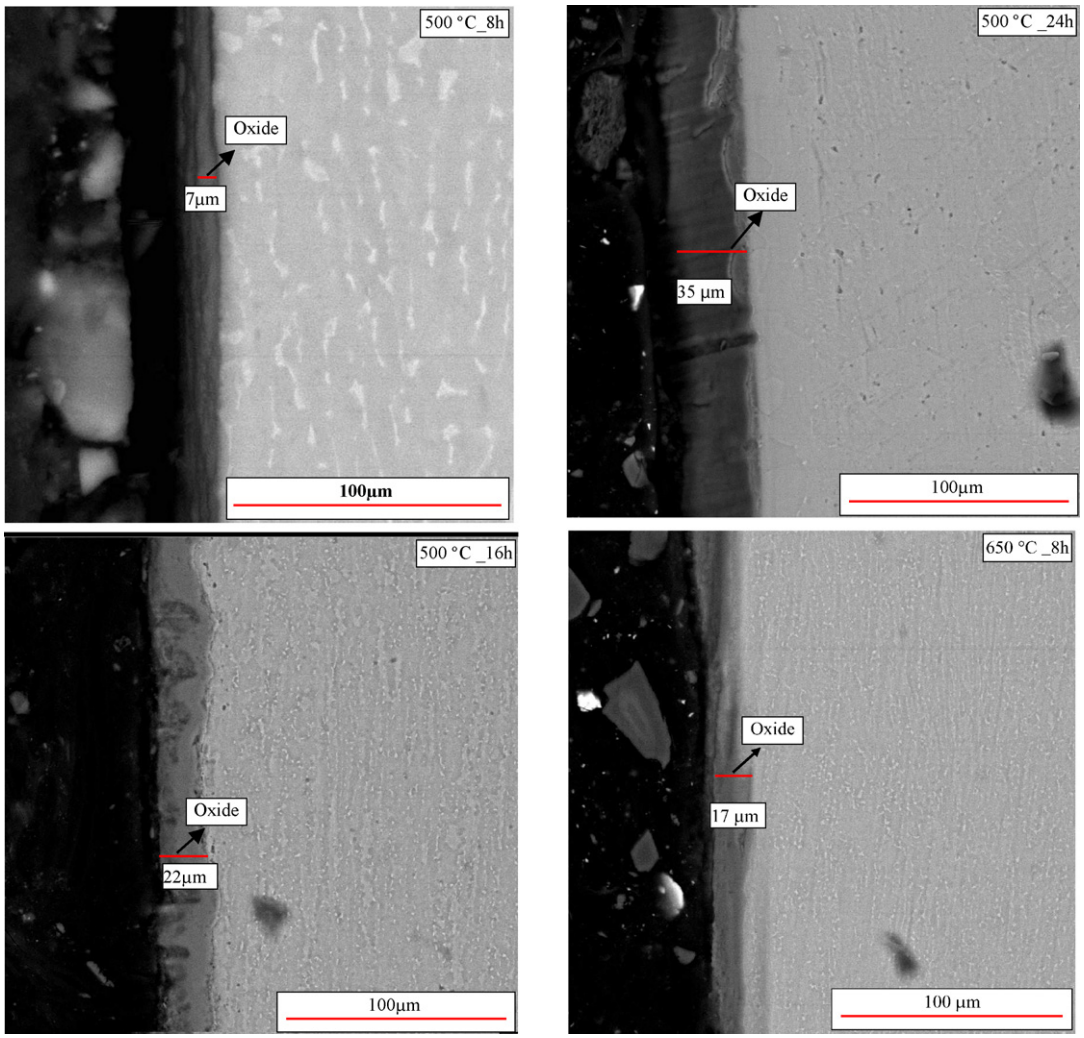

Fig. 5. Cross-sectional scanning electron micrographs of Ti6Al4V alloy samples thermally oxidized at different temperature (500, 650 and 800 °C) for various durations of time in air (8 h, 16 and 24 h) and at 650 °C for 48 h.

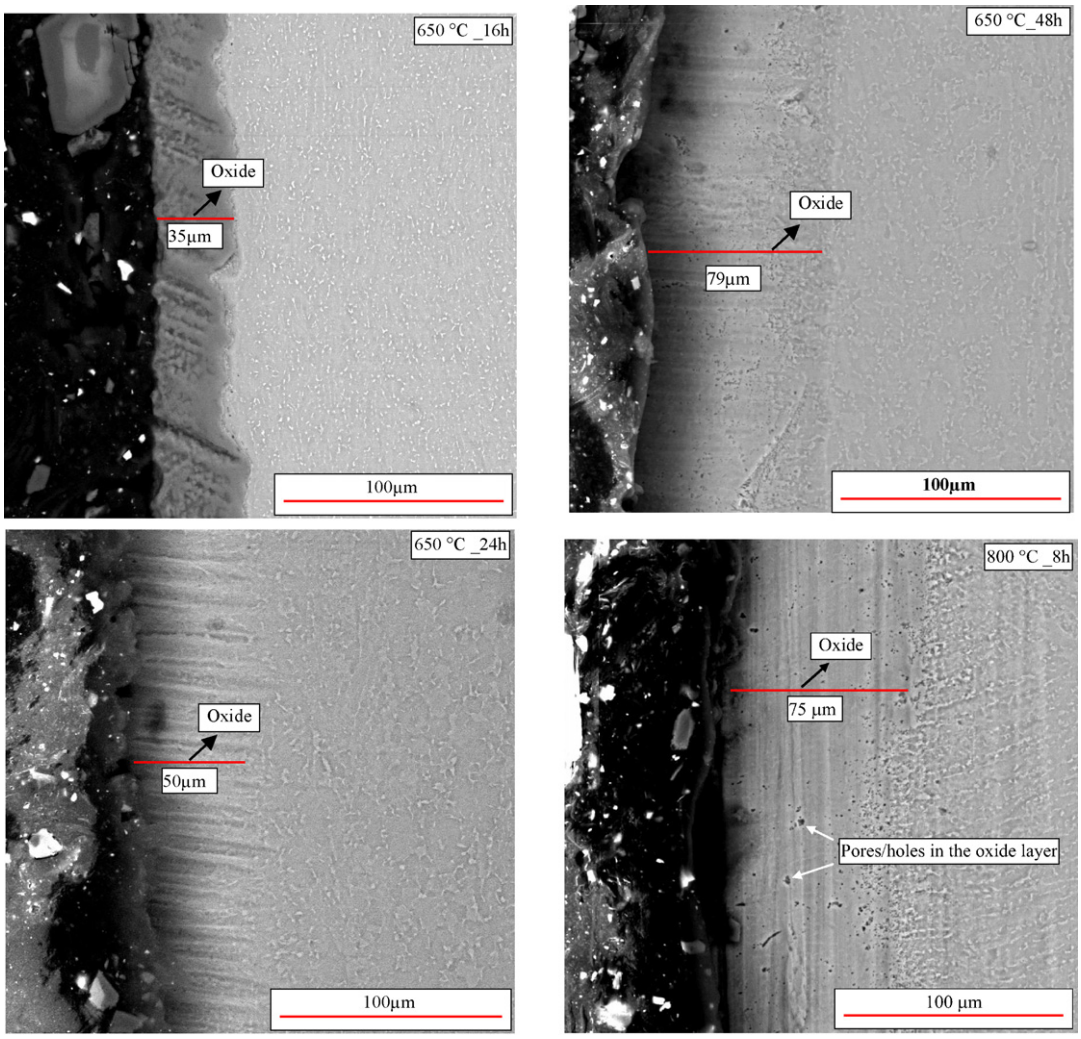

Fig. 5. (*Continued*).

the only dominated phase when the alloy was oxidized at 650 °C for 48 h.

The presence of only the rutile phase on Ti6Al4V oxidized at 800 °C for 8 h suggests the formation of a thick oxide film. The presence of α-Ti and Ti(O) peaks at 500 °C indicates the formation of a thin oxide film whereas the presence of α-Ti, Ti(O) and rutile at 650 °C points out that the thickness of the oxide layer would lie between those oxidized at 500 and 800 °C. The presence of Ti(O) as the strongest peak suggests that rutile formation is minimal at 650 °C, which would otherwise lead to the absence of the Ti(O) peaks [46].

3.5. Microhardness of untreated and thermally oxidized Ti6Al4V alloy

The microhardness of untreated and TO Ti6Al4V alloy measured on the surface of the oxide layer is given in Fig. 7. The microhardness of untreated Ti6Al4V alloy is 324 ± 8 $HV_{0.2}$. Thermally oxidized Ti6Al4V alloy exhibits a significant increase in hardness due to the formation of hard oxide layers and the strains evolved during the dissolution of oxygen beneath the oxide layer of the substrate [47,48]. According to Yan and Wang [49], the low hardness of untreated CP-Ti is due to its relatively low c/a ratio whereas the increase in hardness after thermal oxidation treatment is due to the lattice distortion caused by the dissolved oxygen which is reflected by the increase in c/a ratio. In the present study, the hardness of Ti6Al4V alloy is increased from 324 ± 8 to 985 ± 40 $HV_{0.2}$ when it is thermally oxidized at 650 °C for 48 h, almost a three-fold increase, when compared to that of the untreated sample. However, a lower hardness is observed for the sample oxidized at

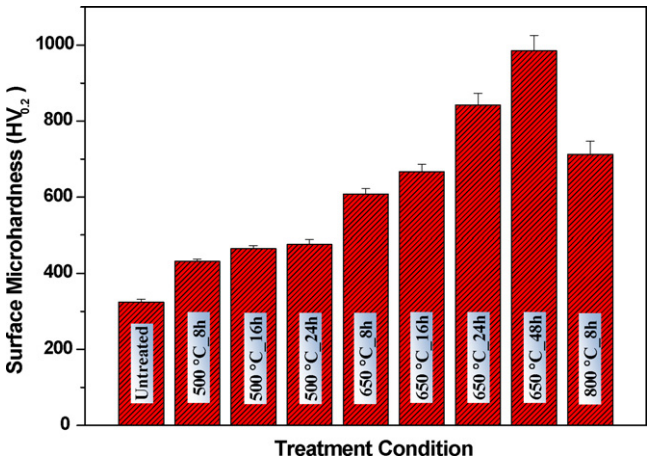

Fig. 7. Surface microhardness of untreated Ti6Al4V alloy and those thermally oxidized at different temperatures for varying duration of time in air.

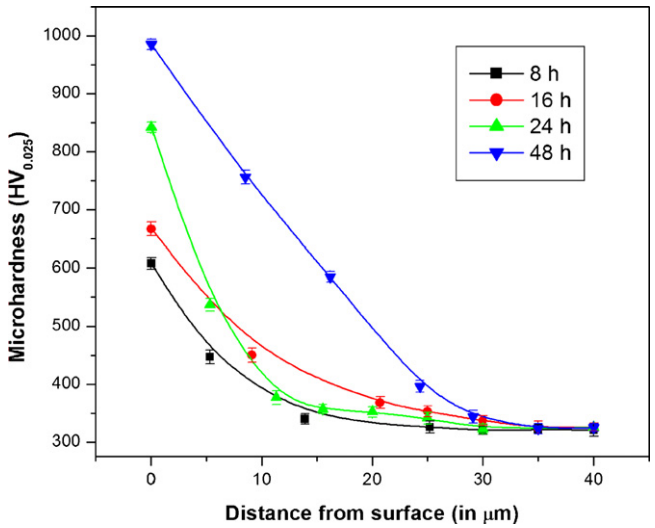

Fig. 8. Microhardness depth profile of Ti6Al4V alloy thermally oxidized at 650 °C for different durations of time in air.

800 °C for 8 h than those treated at 650 °C for 48 h. Guleryuz and Cimenoglu [45] have reported an increase in hardness from 450 to 1300 $HV_{0.01}$ upon oxidation of Ti6Al4V alloy at 600 °C for 60 h. The scattering in microhardness values of thermally oxidized Ti6Al4V alloy appears to increase with increase in oxidation temperature, which is in agreement with the results of Guleryuz and Cimenoglu [45]. This may be due to the microstructural inhomogenities, i.e., the formation of oxide islands with their grains on to the surface. It has been reported elsewhere that TO would lead to an increase in surface roughness of the oxide film due to the differential oxidation rate of individual grains of the polycrystalline alloy [50,51] that supports the results of the present work of higher surface roughness and microhardness with increase in treatment temperature and time. The increase in surface roughness of the oxide could be the contributing factor for the observed scattering in the hardness values. The microhardness depth profile of Ti6Al4V alloy thermally oxidized at 650 °C for 8, 16, 24 and 48 h is given in Fig. 8. The reduction in hardness from the surface to the core is clearly evident. The microhardness of Ti6Al4V alloy thermally oxidized at 650 °C for 8, 16 and 24 h quickly reaches the core hardness value. However, the decrease in hardness is gradual when the alloy is oxidized at 650 °C for 48 h, which may be due to the involvement of the thicker and softer oxygen diffused zone.

3.6. Mechanism of oxide film formation on Ti6Al4V alloy

The oxidation behaviour of titanium has been studied earlier. Titanium has an appreciable solubility of oxygen under normal oxidizing conditions. Titanium reacts immediately with oxygen and forms a thin TiO_2 layer (~4–5 nm thick) on the surface that prevents it from further oxidation or oxygen diffusion at lower temperature. However, at sufficiently high temperatures, oxygen diffuses through the oxide layer, and at the metal–oxide interface, it reacts with titanium to form TiO_2. Formation of an oxide layer is accompanied with the dissolution of diffusing oxygen in the metal beneath it. An increase in temperature accelerates the rate of oxidation, thus allowing the formation of a thicker oxide layer with a deeper oxygen diffusion zone. The oxidation of titanium and its alloys follows different rate laws as a function of temperature. Below 400 °C oxidation of titanium follows a logarithmic rate law whereas a transition from logarithmic to parabolic or an approximately cubic rate law is observed between 400 and 600 °C. The oxidation of titanium follows parabolic rate law between 600 and 700 °C while after

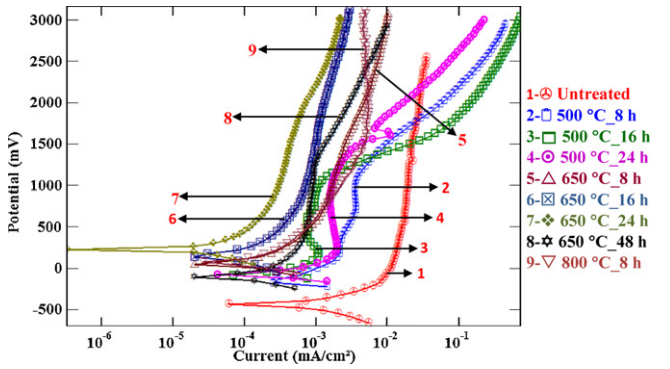

Fig. 9. Potentiodynamic polarization curves of untreated Ti6Al4V alloy and samples thermally oxidized at different temperatures for various durations of time in air.

extended reaction it transforms into an approximately linear rate [51].

In the present study thermal oxidation of Ti6Al4V alloy was performed at 500, 650 and 800 °C. The major alloying elements, viz., Al and V would influence the oxidation behaviour of the Ti6Al4V alloy. It has been reported earlier that Al has reduced the amount of dissolved oxygen from 34 to 0.3 at.% when Ti–Al alloy was oxidized at 700 °C [52]. Since the formation of Al_2O_3 is thermodynamically more favourable, the formation of an α-Al_2O_3 layer near the external interface and distribution of alumina in the distinct sub-layers of variable thickness help reducing the amount of dissolved oxygen [52]. However, addition of 1.4 wt.% of V has been observed to prevent the formation of Al_2O_3 barrier layer at the interface of inner/outer layers and increase the rate of oxidation [53]. Since, the vanadium content of the present sample is more than 1.4 wt.%, the formation of oxygen diffusion layer for samples oxidized at 650 and 800 °C is expected [53]. The EDX analysis of the oxide layer formed on Ti6Al4V alloy of the present study reveals the presence of Ti, Al, V and O, which suggests the formation of oxides of Ti, Al and V (Fig. 4). The formation of oxygen diffusion layer, however, could not be predicted based on the EDX analysis. Based on the elongation of '*c*' axis, increase in lattice parameter and increase in *c*/*a* ratio, Yan and Wang [49] have reported that the formation of oxygen diffusion layer. Ebrahimi et al. [54] have confirmed the presence of dissolved oxygen in titanium based on the broadening of the α-peaks and appearance of a shoulder pattern at lower diffraction angles. The X-ray diffraction pattern of Ti6Al4V alloy thermally oxidized at 650 °C reveals the shift of peaks pertaining to α-Ti to lower diffraction angles, suggesting an increase in lattice parameters. Broadening of the α-peaks and appearance of a shoulder pattern (marked as * in Fig. 6) at lower diffraction angles confirms the presence of oxygen diffusion layers. Hence, thermal oxidation of Ti6Al4V alloy involves simultaneous dissolution and oxide scale formation, leading to the formation of an oxygen diffusion layer. With increase in treatment temperature and time, the thickness of the oxide containing Al_2O_3 and TiO_2, and the oxygen content of the diffusion layer increase and as a result an increase in hardness is observed.

3.7. Potentiodynamic polarization studies of untreated and thermally oxidized Ti6Al4V alloy

The potentiodynamic polarization curves of untreated and TO Ti6Al4V alloy in Ringer's solution in the potential range of −250 to +3000 mV vs. SCE with respect to their OCP are shown in Fig. 9. Though a clinical reality does not exist at such a high potential of +3000 mV vs. SCE, this potential range was chosen to observe the effect of oxidation conditions and consequently the oxide layer thickness on the passivity and breakdown of the oxide layer, if any.

Table 2
Corrosion parameters of untreated and thermally oxidized Ti6Al4V alloy.

Sample	Treatment time (h)	E_{corr} (mV)	i_{corr} (mA cm^{-2})	i_{pass} (mA cm^{-2})[a]	Impedance (kΩ cm^2)
Untreated	0	−433	6.7×10^{-4}	2.1×10^{-2}	10.2
TO at 500 °C	8	−130	2.8×10^{-4}	3.6×10^{-3}	11.5
	16	−84	1.4×10^{-4}	1.1×10^{-3}	15.9
	24	−76	1.9×10^{-4}	1.7×10^{-3}	14.9
TO at 650 °C	8	+59	6.0×10^{-5}	1.7×10^{-3}	60.4
	16	+135	5.7×10^{-5}	7.4×10^{-4}	563.4
	24	+233	1.3×10^{-5}	3.1×10^{-4}	905.2
	48	−105	6.6×10^{-5}	9.1×10^{-4}	73.6
TO at 800 °C	8	+68	6.8×10^{-5}	2.2×10^{-3}	46.7

[a] Measured at +1000 mV from OCP vs. SCE.

The corrosion potential (E_{corr}), corrosion current density (i_{corr}) and the current density corresponding to +1000 mV vs. SCE, measured for the untreated and TO Ti6Al4V alloy are given in Table 2. The thermally oxidized Ti6Al4V alloy sample exhibits a shift in E_{corr} towards the noble direction and a decrease in i_{corr} when compared to that of the untreated alloy sample. The E_{corr} and i_{corr} values vary with the temperature and time duration employed for oxidation. The Ti6Al4V alloy thermally oxidized at 650 °C for 24 h exhibits a nobler E_{corr} and lower i_{corr} values among all sample studied (Fig. 9 and Table 2). The E_{corr} of Ti6Al4V alloy samples oxidized at 500 °C is negative while those oxidized at 650 °C are positive (except those oxidized for 48 h). This is due to the increase in thickness of the oxide layer and decrease in the gaps/uncovered areas between the oxide layer for those oxidized at 650 °C for 8, 16 and 24 h.

The anodic branch of the polarization curve exhibits an active–passive transition in all the cases. However, the active region of the polarization curves of the thermally oxidized Ti6Al4V alloy is extended towards lower current region, suggesting the ability of the thermally formed oxide layer to offer an improvement in corrosion resistance. The decrease in i_{pass} of thermally oxidized Ti6Al4V alloy suggests that the oxide film formed on its surface possesses a better insulating property and hinders the passage of higher current for further chemical reaction/oxidation of species in the electrolyte compared to that of the naturally formed thin oxide layer (∼5 nm) present on the untreated alloy (Fig. 9 and Table 2). The i_{pass} of the Ti6Al4V alloy oxidized at 650 °C for 24 h is the lowest and it is about 67 times lower when compared to that of untreated one.

Several researchers have confirmed that thermally oxidized CP-Ti and Ti6Al4V alloy offer a better corrosion resistance when compared to their untreated counterparts in a variety of environments. Garcia-Alonso et al. [36] have reported that the i_{pass} of Ti6Al4V alloy, thermally oxidized at 500 and 700 °C for 1 h, in Ringer's solution, is very low when compared to that of the untreated alloy. A comparison of the i_{pass} of thermally oxidized Ti6Al4V alloy reported by Garcia-Alonso et al. [36] and those observed in the present study reveals that the extent of decrease in i_{pass} following oxidation is relatively higher in the present study. This is due to the variation in the thickness of the oxide film following the difference in the treatment time employed—about 1 h by Garcia-Alonso et al. [36] whereas a minimum of 8 h in the present study. Guleryuz and Cimenoglu [27] have reported that Ti6Al4V alloy thermally oxidized at 600 °C offers excellent corrosion resistance when compared to untreated alloy when they are subjected to accelerated corrosion test in 5 M HCl. According to them, the formation of a thick and stable oxide film on the surface of the alloy results in a negligible loss in weight even after 36 h of immersion in 5 M HCl. Bloyce et al. [33] have compared the corrosion resistance of untreated, plasma nitrided (PN), thermally oxidized (TO), palladium-treated thermally oxidized (PTO) CP-Ti in 3.5% NaCl solution at room temperature by potentiodynamic polarization studies. Both TO and PTO CP-Ti samples exhibit a shift in E_{corr} towards the noble direction and a decrease in i_{corr} compared to that of PN and untreated CP-Ti. They have also evaluated the corrosion resistance of these samples by the accelerated corrosion test that involves immersion in boiling 20% HCl. Both TO and PTO CP-Ti samples increase the lifetime by a factor of about 13 and 27, respectively compared to PN CP-Ti. The results of the present study further confirm the fact that thermally oxidized Ti6Al4V alloy could offer excellent corrosion resistance compared to untreated samples. Though both i_{corr} and i_{pass} are indicative of the corrosion protective ability, in the present study i_{pass} is used to rank the thermally oxidized Ti as it reflects the ability of a material/treatment to sustain in an aggressive environment even at higher anodic potentials. Based on the i_{pass} values, the ability of untreated and thermally oxidized Ti6Al4V alloy of the present study to offer a better corrosion resistance can be ranked as follows: untreated < TO at 500 °C for 8 h < TO at 800 °C for 8 h < TO at 500 °C for 24 h = TO at 650 °C for 8 h < TO at 500 °C for 16 h < TO at 650 °C for 48 h < TO at 650 °C for 16 h < TO at 650 °C for 24 h. This ranking indicates that the corrosion protective ability of thermally oxidized Ti6Al4V alloy does not follow a linear relation either with treatment temperature or time. This may be due to the defects present in the oxide layer. An extensive study of the defects and volume of pores formed as a function of temperature and time employed for oxidation will provide a better understanding of this phenomenon.

3.8. Electrochemical impedance spectroscopic studies of untreated and thermally oxidized Ti6Al4V

The Bode impedance plots of untreated and TO Ti6Al4V alloy in Ringer's solution, at their respective OCP's, are shown in Fig. 10(a). The Bode impedance plot reveals that the impedance values of thermally oxidized Ti6Al4V alloy are higher than that of the untreated alloy (Fig. 10(a)). The Bode impedance plots of Ti6Al4V alloy subjected to TO 650 and 800 °C are at the higher side in the entire frequency range studied while those oxidized at 500 °C are at the higher side at higher frequency region when compared to the untreated alloy sample. A direct correlation between thickness of the oxide layer obtained as a function of temperature and time employed for oxidation and the impedance values could not be established. This may be due to the presence of gaps/discontinuities between the oxide grains.

The Bode phase angle plots (Fig. 10(b)) exhibit much variation, which provides an understanding of the corrosion mechanism. Untreated Ti6Al4V alloy exhibits a phase angle maximum of −75° at an intermediate frequency of 90 Hz, which remains constant over a wide frequency range, from 90 to 8 Hz and subsequently declines to −18° at lower frequencies. The Ti6Al4V alloy sample oxidized at 500 °C exhibits a relatively lower phase angle maximum of about −60°, which remains constant over a wide frequency range. The occurrence of a constant phase angle maximum over a wide frequency range is typical of passive surfaces, which indicates

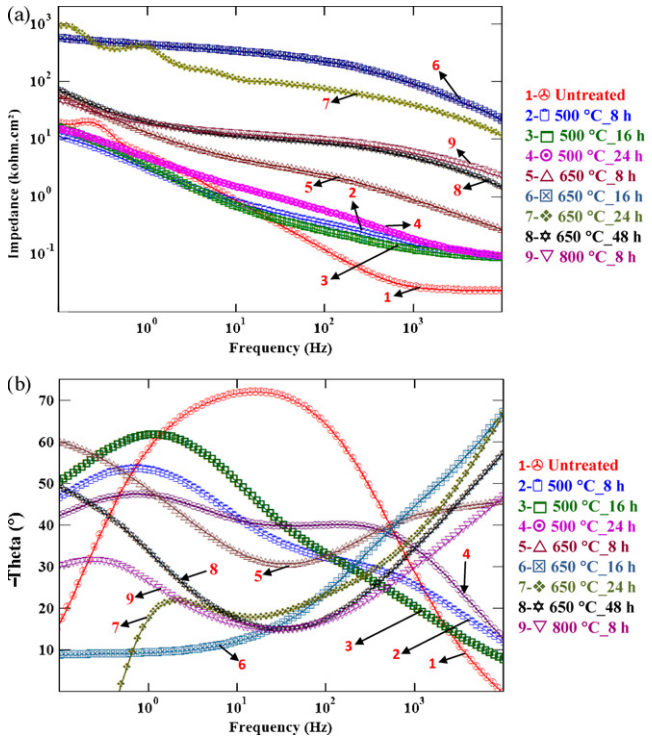

Fig. 10. (a) Bode impedance plots of untreated Ti6Al4V alloy and samples thermally oxidized at different temperatures for various durations of time in air. (b) Bode phase angle plots of untreated Ti6Al4V alloy and samples thermally oxidized at different temperatures for various durations of time in air.

a near capacitive behaviour. Such an occurrence also describes the dielectric properties of the oxide film; the difficulty encountered in charge transfer process and, ascertains a good corrosion protective ability of the oxide film. The phase angle plots of Ti6Al4V alloy thermally oxidized at 650 °C for 48 h and at 800 °C for 8 h starts from −57° and −47° at 10,000 Hz, gradually decrease to −15°, at an intermediate frequency of around 50 Hz and further increases to −50° and −30°, respectively. The continuous decrease of the phase shift of Bode phase angle curves can be explained using a transmissive boundary model, which considers the fact that only the bottom of the hole is conducting whereas its wall is isolating [55]. The Bode phase angle plots of some of the thermally oxidized Ti6Al4V alloy exhibit two inflexion points in the frequency range studied, suggesting the involvement of the mass transfer through pores. The occurrence of two inflections in the phase angle plot indicates the involvement of two time constants, which has also been reported earlier by Garcia-Alonso et al. [36] for Ti6Al4V alloy oxidized at 700 °C for 1 h. The observed variation in the curves suggests a strong dependence of the nature of the oxide layer and the presence of gaps/discontinuities rather than on the temperature and time employed for oxidation. The increase in impedance values of thermally oxidized Ti6Al4V alloy suggests an excellent corrosion protective ability and support the observations made by potentiodynamic polarization studies. For the Ti6Al4V alloy thermally oxidized at 650 °C for 24 h, the increase in impedance value is almost 90 times when compared to that of the untreated alloy, which confirms its ability to offer an excellent corrosion resistance.

The results of the polarization and EIS studies reveal that the corrosion protective ability of the Ti6Al4V alloy is improved when it is thermally oxidized. The excellent chemical resistance of the rutile phase [56] could be one of the contributing factors in samples oxidized at 650 and 800 °C. There is no direct correlation between the thickness of the oxide layer obtained as a function of temperature and time employed for oxidation and the corrosion protective ability; rather it appears to be a function of the nature of the oxide layer and the presence of gaps/discontinuities in it.

4. Conclusions

The oxidation behaviour of Ti6Al4V alloy at 500, 650 and 800 °C for 8, 16, 24 and 48 h, was evaluated based on their surface morphology, surface roughness, structural characteristics and hardness. The mechanism of formation of the oxide layer on Ti6Al4V alloy was discussed. The corrosion behaviour of thermally oxidized Ti6Al4V alloy in Ringer's solution was compared with that of the untreated alloy. The study leads to the following conclusions:

- The surface morphology of thermally oxidized Ti6Al4V alloy reveals the formation of a thin adherent surface layer at 500 °C that changes into a small grain structure at 650 °C and a complete coverage of oxide islands with the grains oriented perpendicular to the substrate at 800 °C. The growth mode involves the formation of a thin oxide scale followed by its agglomeration and growth to completely cover the surface.
- Thermal oxidation of Ti6Al4V alloy performed at 800 °C for 16 and 24 h exhibits spalling of the oxide layer.
- Ti6Al4V alloy oxidized at 800 °C exhibits the formation of a thick oxide film that consists of only the rutile phase whereas both TiO and α/β-Ti are found to be present on Ti6Al4V alloy oxidized at 500 and 650 °C, with TiO as the dominant phase at 650 °C. Anatase phase peaks are observed for the sample thermally oxidized at 500 °C.
- Almost a threefold increase in hardness is observed for Ti6Al4V alloy oxidized at 650 °C for 48 h compared to that of the untreated alloy (324 ± 8 $HV_{0.2}$).
- The E_{corr}, i_{corr}, i_{pass} and impedance values indicate that corrosion protective ability of thermally oxidized Ti6Al4V alloy is much better than the untreated alloy. Based on the i_{pass} value, the corrosion protective ability of untreated and thermally oxidized Ti6Al4V alloy of the present study can be ranked as follows: untreated > TO at 500 °C for 8 h > TO at 800 °C for 8 h > TO at 500 °C for 24 h = TO at 650 °C for 8 h > TO at 500 °C for 16 h > TO at 650 °C for 48 h > TO at 650 °C for 16 h > TO at 650 °C for 24 h.
- There is no direct correlation between the thickness of the oxide layer obtained as a function of temperature and time employed for oxidation and the corrosion protective ability; rather it appears to be a function of the nature of the oxide layer and the presence of gaps/discontinuities in it.

Acknowledgement

The authors express their sincere thanks to Prof. S.P. Mehrotra, Director, National Metallurgical Laboratory, Jamshedpur, for his keen interest and permission to publish this paper.

References

[1] P. Kovacs, J.A. Davidson, Chemical and electrochemical aspects of the biocompatibility of titanium and its alloys, in: S.A. Brown, J.E. Lemons (Eds.), Medical Applications of Titanium and its Alloys: The Materials and Biological Issues, 1996, ASTM STP 1272, p. 163.
[2] J.A. Hunt, M. Stoichet, Curr. Opin. Solid State Mater. Sci. 5 (2001) 161.
[3] D.F. Williams, Titanium and titanium alloys, in: D.F. Williams (Ed.), Biocompatibility of Clinical Implant Materials, vol. II, CRC Press, 1981, p. 9.
[4] M.J. Long, H.J. Rack, Biomaterials 19 (1998) 1621.
[5] Y. Mu, T. Kobayashi, M. Sumita, A. Yamamoto, T. Hanawa, J. Biomed. Mater. Res. 49 (2000) 238.
[6] P.A. Lilley, P.S. Walker, G.W. Blunn, Transactions of the 4th Word Biomaterials Congress, Berlin, April 24–28, 1992, p. 227.
[7] R. Thull, M. Schaldach, Springer-Verlag, Corrosion of highly stressed orthopaedic joint replacements. New York/Heidelberg/Berlin 1976, p. 242.
[8] S.A. Brown, P.J. Hughes, K. Merrit, J Orthop. Res. 6 (1988) 572.
[9] D.W. Hoeppner, V. Chandrasekaran, Wear 173 (1994) 189.

[10] L.M. Rabbe, J. Rieu, A. Lopez, P. Combrade, Clin. Mater. 15 (1994) 221.
[11] S. Rao, T. Ushida, T. Tateishi, Y. Okazaki, S. Asao, Biomed. Mater. Eng. 6 (1996) 79.
[12] P.R. Walker, J. Leblanc, M. Sikorska, Biol. Chem. 28 (1990) 3911.
[13] S. Yumoto, H. Ohashi, H. Nagai, S. Kakimi, Y. Ogawa, Y. Iwata, H. Ishii, Int. J. PIXE 2 (1992) 493.
[14] W.F. Ho, C.P. Ju, H. Chern Lin, Biomaterials 20 (1999) 2115.
[15] M.F. Semlitsch, H. Weber, R.M. Streicher, R. Schon, Biomaterials 13 (1992) 781.
[16] J. Zwicker, U. Etzold, Th. Moser, Abrasive properties of oxide layers on Ti-Al15-Fe2.5 in contact with high density polyethylene Titanium'84 Science and Technology, vol. 2, Deutsche Gesellschaft Fur Metallkunde EV, 2, Munich, 1985, p. 1343.
[17] D.P. Perl, A.R. Brody, Science 208 (1980) 297.
[18] D.R. Crapper, D.R. McLachlan, B. Farnell, H. Galin, S. Karlik, G. Eichhorn, U. De Boni, Aluminum in human brain disease, in: B. Sarkar (Ed.), Biological Aspects of Metals and Metals-Related Diseases, Raven Press, New York, 1993, p. 209.
[19] C. Sittig, M. Textor, N.D. Spencer, M. Wieland, P.H. Vallotton, J. Mater. Sci. Mater. Med. 10 (1) (1999) 35.
[20] H.B. Wen, J.G. Wolke, J.R. Wijn, Q. Liu, F.Z. Cui, K. de Groot, Biomaterials 18 (1997) 1471.
[21] X. Nie, A. Leyland, A. Matthews, Surf. Coat. Technol. 149 (2002) 245.
[22] T. Brendel, A. Engel, C. Russel, J. Mater. Sci. Mater. Med. 3 (3) (1992) 175.
[23] P. Andreazza, M.I. De Barros, C. Andreazza-Vignolle, D. Rats, L. Vandenbulcke, Thin Solid Films 319 (1998) 62.
[24] M. Uchida, N. Nihira, A. Mitsuo, K. Toyoda, K. Kubota, T. Aizawa, Surf. Coat. Technol. 177–178 (2004) 627.
[25] S.W.K. Kweh, K.A. Khor, P. Cheang, Biomaterials 23 (3) (2002) 775.
[26] T. Hanawa, Y. Kamiura, S. Yamamoto, T. Kohgo, A. Amemiya, H. Ukai, K. Murakami, K. Asaoka, J. Biomed. Mater. Res. 36 (1997) 131.
[27] H. Guleryuz, H. Cimenoglu, Biomaterials 25 (2004) 3325.
[28] M.F. Lopez, J.A. Jimenez, A. Gutierrez, Electrochim. Acta 48 (2003) 1395.
[29] D. Velten, V. Biehl, F. Aubertin, B. Valeske, W. Possart, J. Breme, J. Biomed. Mater. Res. 59 (2002) 18.
[30] M.L. Escudero, J.L. Gonzalez-Carrasco, C. Garcıa-Alonso, E. Ramırez, Biomaterials 16 (1995) 735.
[31] D. Siva Rama Krishna, Y.L. Brama, Y. Sun, Tribol. Int. 40 (2007) 329.
[32] C. Munuera, T.R. Matzelle, N. Kruse, M.F. Lopez, A. Gutierrez, J.A. Jimenez, C. Ocal, Acta Biomater. 3 (2007) 113.
[33] A. Bloyce, P.Y. Qi, H. Dong, T. Bell, Surf. Coat. Technol. 107 (1998) 125.
[34] N.D. Tomashov, P.M. Altovskii, Corrosion and Protection of Titanium, Government Scientific–Technical Publication of Machine-Building Literature, Moscow, 1963.
[35] R.W. Schutz, L.C. Covington, Corrosion 37 (1981) 585.
[36] M.C. Garcia-Alonso, L. Saldana, G. Valles, J.L. Gonzalez-Carrasco, J. Gonzalez–Cabrero, M.E. Martinez, E. Gil-Garay, L. Munuera, Biomaterials 24 (2003) 19.
[37] H. Dong, A. Bloyce, P.H. Morton, T. Bell, Titanium'95 Science and Technology, 1995, p. 1999.
[38] G.P. Burns, J. Appl. Phys. 65 (5) (1989) 2095.
[39] C. Boettcher, Surf. Eng. 16 (2) (2000) 148.
[40] H.L. Du, P.K. Datta, D.B. Lewis, J.S. Burnell-Gray, Corros. Sci. 36 (1994) 631.
[41] R.W. Schutz, D.E. Thomas, Corrosion of Titanium and Titanium Alloys, ASM Handbook, Corrosion, vol. 13, ASM International, 1987, p. 671.
[42] H. Dong, A. Bloyce, P.H. Morton, T. Bell, Surf. Eng. 13 (1997) 402.
[43] G. Bertrand, K. Jarraya, J.M. Chaix, Oxid. Met. 21 (1983) 1.
[44] F. Borgioli, E. Galvanetto, F. Iozzelli, G. Pradelli, Mater. Lett. 59 (2005) 2159.
[45] H. Guleryuz, H. Cimenoglu, Surf. Coat. Technol. 192 (2005) 164.
[46] C.C. Ting, S.Y. Chen, D.M. Liu, Thin Solid Films 402 (2002) 290.
[47] S. Weissman, A. Shrier, in: R.I. Jaffee, N.E. Promisel (Eds.), The Science, Technology and Application of Titanium, Pergamon Press, London, 1968, p. 441.
[48] F. Borgioli, E. Galvanetto, F.P. Galliano, T. Bacci, Surf. Coat. Technol. 141 (2001) 103.
[49] W. Yan, X.X. Wang, J. Mater. Sci. Lett. 39 (2004) 5583.
[50] P.A. Dearnley, K.L. Dahm, H. Çimenoglu, Wear 256 (2004) 469.
[51] P. Kofstad, High Temperature Corrosion, Elsevier Applied Science, Essex, 1988.
[52] A.M. Chaze, C. Coddet, J. Less Common Met. 157 (1990) 55.
[53] S. Becker, A. Rahmel, M. Schorr, M. Schutze, Oxid. Met. 38 (1992) 425.
[54] A.R. Ebrahimi, F. Zarei, R.A. Khosroshahi, Surf. Coat. Technol. 203 (2008) 199.
[55] Y. Mueller, R. Tognini, J. Mayer, S. Virtanen, J. Biomed. Mater. Res. 82A (2007) 936.
[56] A. Wisbey, P.J. Gregson, L.M. Peter, M. Tuke, Biomaterials 12 (1991) 470.